Vacuum 85 (2010) 263–267

Contents lists available at ScienceDirect

Vacuum

journal homepage: www.elsevier.com/locate/vacuum

Effects of sputtering pressure and Al buffer layer thickness on properties of AZO films grown by rf magnetron sputtering

C.H. Tseng [a], W.H. Wang [b], H.C. Chang [b], C.P. Chou [a], C.Y. Hsu [b,*]

[a] Department of Mechanical Engineering, National Chiao Tung University, Taiwan, ROC
[b] Department of Mechanical Engineering, Lunghwa University of Science and Technology, Taoyuan, Taiwan, ROC

A R T I C L E I N F O

Article history:
Received 14 October 2009
Received in revised form
17 June 2010
Accepted 22 June 2010

Keywords:
Transparent conductive oxide
Al buffer layer
Rf magnetron sputtering
Electrical resistivity

A B S T R A C T

Transparent and conductive Al-doped (2 wt.%) zinc oxide (AZO) films were deposited on inexpensive soda-lime glass substrates by using rf magnetron sputtering at room temperature. This study analyzed the effects of argon sputtering pressure, which varied in the range from 0.46 to 2.0 Pa, on the morphological, electrical and optical properties of AZO films. The only (0 0 2) diffraction peak of the film were observed at $2\theta \sim 34.45^{\circ}$, exhibiting that the AZO films had hexagonal ZnO wurtzite structure, and a preferred orientation with the *c*-axis perpendicular to the substrate. By applying a very thin aluminum buffer layer with the thickness of 2 nm, findings show that the electrical resistivity was 9.46×10^{-4} Ω-cm, and the average optical transmittance in the visible part of the spectra was approximately 81%. Furthermore, as for 10 nm thick buffer layer, the electrical resistivity was lower, but the transmittance was decreased.

© 2010 Elsevier Ltd. All rights reserved.

1. Introduction

Transparent conducting zinc oxide (ZnO) films have been studied extensively because of their good optical characteristics, high stability, excellent electrical properties and low material cost. They also have attracted attention because of their great potential for application in solar cells, surface acoustic wave devices, piezoelectric transducers and optoelectronic devices etc [1]. ZnO has a wide and direct band gap of 3.37 eV at room temperature, and is optically transparent like indium oxide and tin oxide [2]. Non-doped ZnO usually presents a high resistivity due to a low carrier concentration [3]. In order to increase its electrical and optical properties, ZnO is commonly doped with Group III elements, such as boron (B), indium (In), aluminum (A1) and gallium (Ga). Among these impurity doped zinc oxide films, Al-doped zinc oxide (AZO) thin film is considered an excellent candidate material [4]. Al presents a very high reactivity leading to oxidation during the growth of films, and exhibits a wide band gap, high transparency, low resistivity, non-toxicity, low cost, and stability in hydrogen plasma compared with ITO and SnO_2 [5].

Several techniques have been developed in the deposition of AZO films, which is the most commonly used radio frequency (rf) magnetron sputtering [6]. The most important deposition parameters that should be controlled in order to develop AZO films with the desired properties are the substrate-to-target distance, the substrate temperature, the oxygen flow rate, the rf power, and the working pressure [7]. In this study, we examine the argon gas pressure dependence of the electrical, structural and optical properties of AZO transparent conductive films deposited on glass substrates. In order to improve the quality of the AZO films, the effects of Al buffer layers are also investigated.

2. Experimental procedures

Al-doped ZnO films were deposited onto soda-lime glass substrates with dimensions of 20 × 20 × 1 mm by rf magnetron sputtering in an argon gas atmosphere. The glass substrates were ultrasonically cleaned in a detergent bath, and then cleaned with isopropyl alcohol, acetone and distilled water, and blow-dried with nitrogen. A commercially available hot-pressed and sintered disc of ZnO (purity, 99.99%) mixed with 2 wt.% Al_2O_3 (purity, 99.99%), 51.2 mm in diameter, was used as a target (Elecmat, USA). Before coating, the target was pre-sputtered for 10 min to remove any contamination.

The sputtering deposition was performed under an rf power of 100 W and the film thickness was 250 nm on average for all the samples. The flow rate of the argon was controlled by a mass flow controller (MFC) from 33 sccm to 193 sccm, which corresponds to

* Corresponding author. Fax: +886 2 82094845.
E-mail address: cyhsu@mail.lhu.edu.tw (C.Y. Hsu).

0042-207X/$ – see front matter © 2010 Elsevier Ltd. All rights reserved.
doi:10.1016/j.vacuum.2010.06.006

Table 1
Experimental conditions of AZO (with and without buffer layer).

Substrate	Soda-lime glass (20 × 20 × 1 mm)
Target	$ZnO:Al_2O_3$ (98:2 wt.%); 99.995% purity; 51.2 mm diameter
Gas	argon (99.995%)
Base pressure	6.6×10^{-4} Pa
Substrate rotate vertical axis	20 rpm
Substrate-to-target distance	100 mm
Substrate temperature	room temp.
Rf power	100 W
AZO thickness	250 nm
Sputtering pressure	0.46, 0.66, 0.99, 1.3 and 2.0 Pa

Table 2
Deposition parameters of Al buffer.

Substrate	Soda-lime glass (20 × 20 × 1 mm)
Target	Al; 99.99% purity; 51.2 mm diameter
Gas	argon (99.995%)
Base pressure	6.6×10^{-4} Pa
Substrate rotate vertical axis	20 rpm
Substrate-to-target distance	100 mm
Substrate temperature	room temp.
Rf power	50 W
Sputtering pressure	0.99 Pa
Deposition rate	3.96 nm/min
Buffer thickness	2, 5, 10 nm

a sputtering pressure varying from 0.46 to 2.0 Pa. The target to substrate distance was kept at 100 mm and the base pressure was 6.6×10^{-4} Pa Table 1 lists the experimental conditions of the AZO film. In addition, Table 2 lists the sputtering conditions for the Al buffer. As shown in Table 2, the rf powers were 50 W, the sputtering pressure was 0.99 Pa, and the buffer thicknesses were measured to be 2, 5, and 10 nm. The deposition rate of the Al buffer was 3.96 nm/min.

The film thickness was measured using a surface profilometer (α-step, AMBIOS XP-1). A field emission scanning electron microscope (SEM, JEOL, JSM-6500F) analyzed the surface morphologies and an atomic force microscope (AFM, PSIA-XE-100) obtained topographic images. The structural properties were determined by X-ray diffraction (Rigaku-2000 X-ray Generator) using Cu Kα radiation with an angle incidence of 1°. The electrical resistivity was measured by the four-point probe method (Mitsubishi chemical MCP-T600). A UV–vis spectrophotometer carried out optical transmittance measurement in a wavelength range of 300–800 nm.

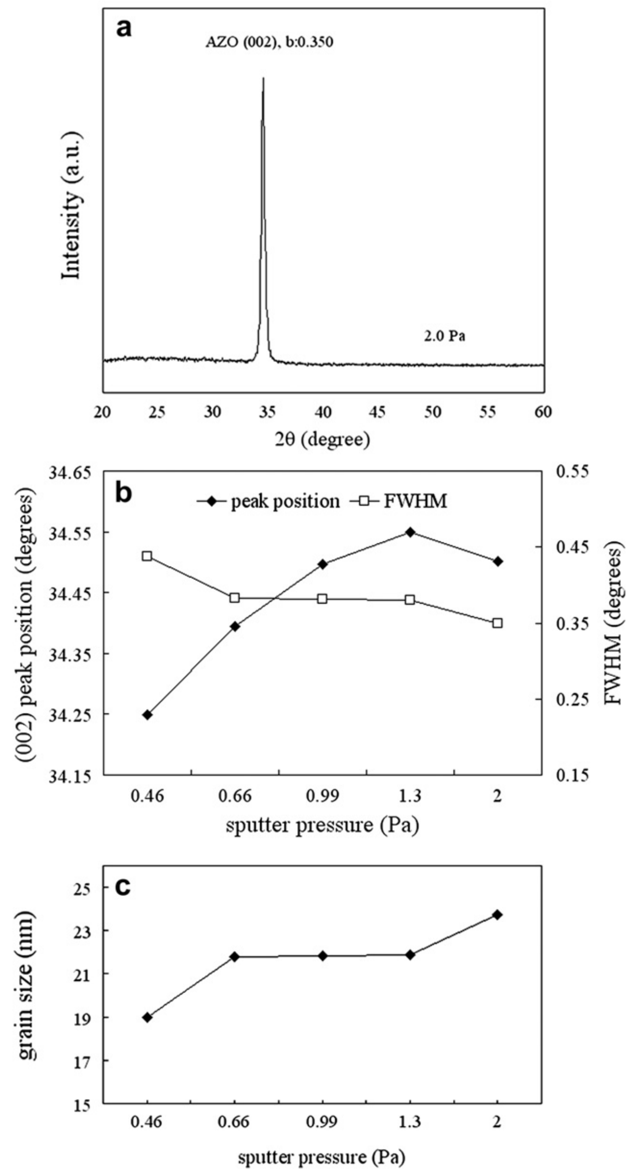

Fig. 2. (a) X-ray curve, (b) variation of peak position and FWHM of the (0 0 2) peak, and (c) grain size plotted as a function of sputter pressure, for 250 nm thick AZO films grown on glass.

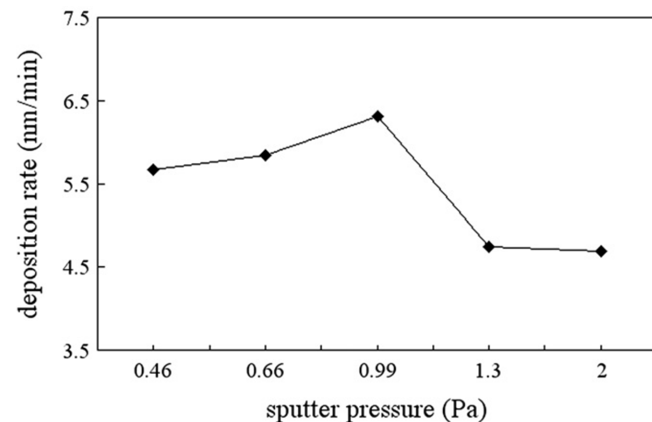

Fig. 1. Deposition rate of AZO films as a function of sputter pressure.

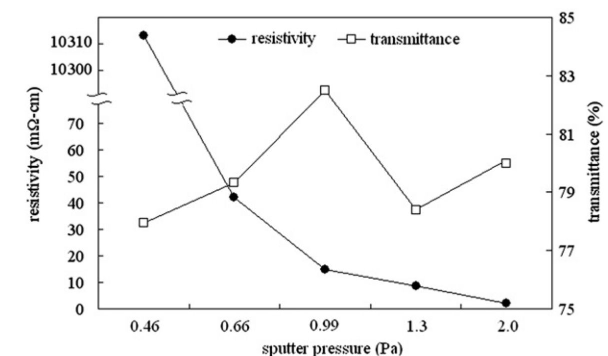

Fig. 3. Electrical resistivity and optical transmittance as a function of sputter pressure, for 250 nm thick AZO films grown on glass deposited at room temperature.

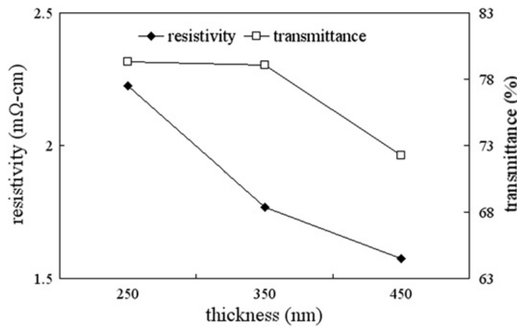

Fig. 4. Electrical resistivity and optical transmittance of AZO films grown on glass as a function of AZO film thickness under the sputter pressure of 2.0 Pa.

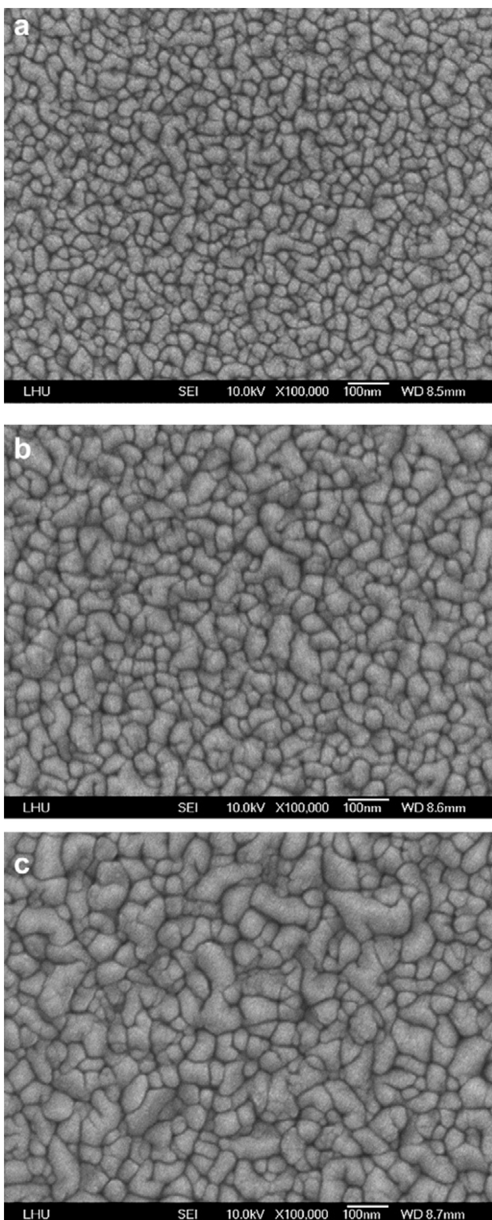

Fig. 5. SEM micrographs of AZO films grown on glass for the sputter pressure of 2.0 Pa, and with different thicknesses (a) 250 nm, (b) 350 nm, and (c) 450 nm.

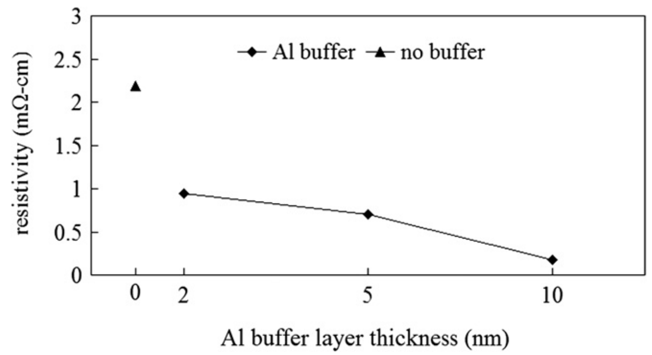

Fig. 6. Resistivity of AZO films grown on Al/glass and glass as a function of buffer thickness, when the AZO films' thickness was 250 nm and the sputter pressure was 2.0 Pa.

3. Results and discussion

The deposition rates of AZO films as a function of sputter pressure are plotted in Fig. 1. As the deposition pressure increases, the deposition rate increases, reaching the maximum value of

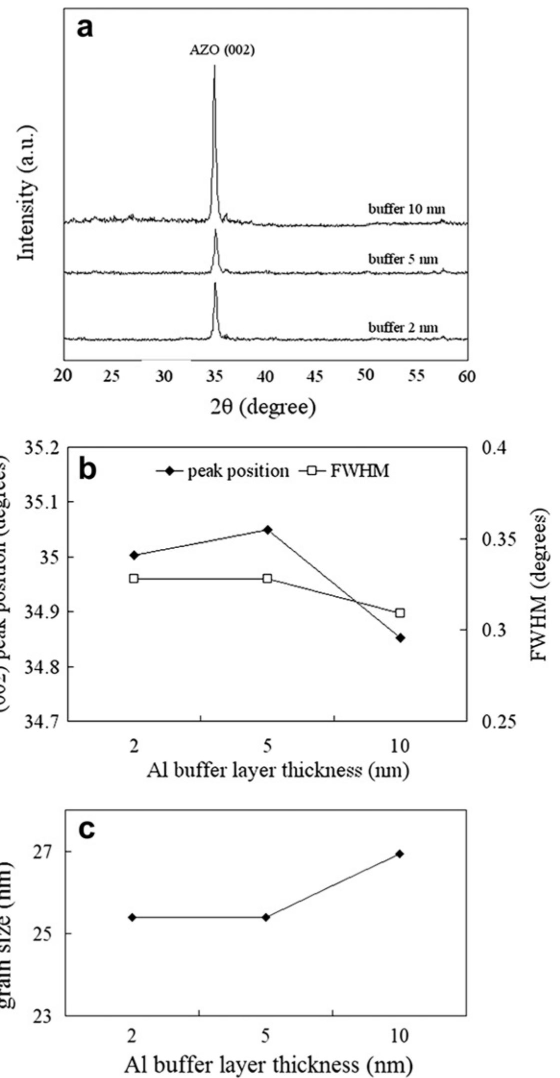

Fig. 7. (a) X-ray curve, (b) variation of peak position and FWHM of the (0 0 2) peak, and (c) grain size plotted as a function of Al buffer thickness, when the AZO films' thickness was 250 nm and the sputter pressure was 2.0 Pa.

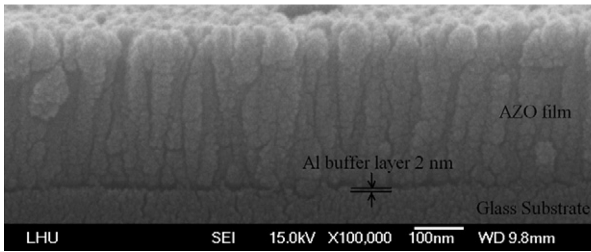

Fig. 8. Cross-sectional SEM image of AZO film when the Al buffer layer thickness was 2 nm.

6.306 nm/min at the deposition pressure of 0.99 Pa, and then decreases with further increase in the sputtering pressure. This is also similar to the results of Ma et al. [8].

Fig. 2 (a) shows the XRD pattern of 250 nm thick AZO films grown on glass at a 2.0 Pa sputter pressure. The experimental results show that there is no significant change in the orientation of all the films deposited in different sputter pressures. The (0 0 2) peak positions and the full width at half maximum (FWHM) of XRD for AZO films vary depending on the sputter pressure as shown in Fig. 2 (b). This reveals the diffraction peak position of 2θ shifts from 34.25° at 0.46 Pa sputter pressure up to a higher angle of 34.55° at a sputter pressure of 1.3 Pa and then decreases to 34.50° at a sputter pressure of 2.0 Pa. The FWHM of XRD depends on the crystalline quality of each grain and distribution of grain orientation [9]. With the increase of sputter pressure, we gradually observed a decrease in the FWHM of XRD for AZO films. The grain size was calculated using Scherrer's formula. The grain sizes of the AZO thin films at different sputter pressures are shown in Fig. 2. (c). The result is consistent with the result of the FWHM of XRD as shown in Fig. 2. (b). This shows that the best quality crystallization of the AZO films should be deposited at a sputter pressure of 2.0 Pa.

Fig. 3 shows the electrical resistivity and optical transmittance as a function of sputter pressure for the AZO films (experimental conditions lists in Table 1). The samples deposited at the sputter pressure increase from 0.46 to 0.66 Pa, causing a steep decrease in the electrical resistivity from 10.32 down to 4.22×10^{-2} Ω-cm. The electrical resistivity then decreases slowly as the sputter pressure further increases. The average transmittance in the visible range is approximately 80% for the sputter pressure of 2.0 Pa. For comparison purposes, Fig. 4 shows the electrical resistivity and optical transmittance at different AZO thicknesses for the sputter pressure

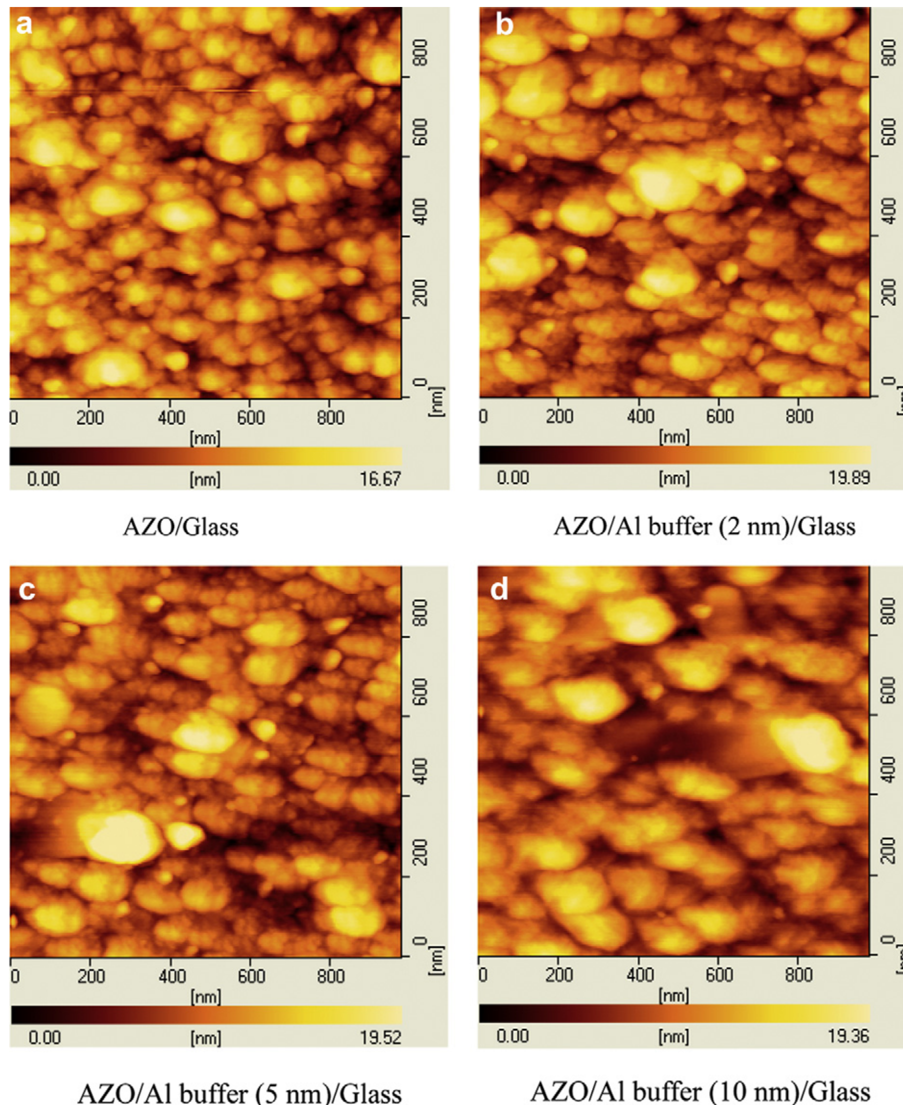

Fig. 9. AFM images of the films corresponding to Fig. 7. (a) AZO/Glass (b) AZO/Al buffer (2 nm)/Glass (c) AZO/Al buffer (5 nm)/Glass (d) AZO/Al buffer (10 nm)/Glass.

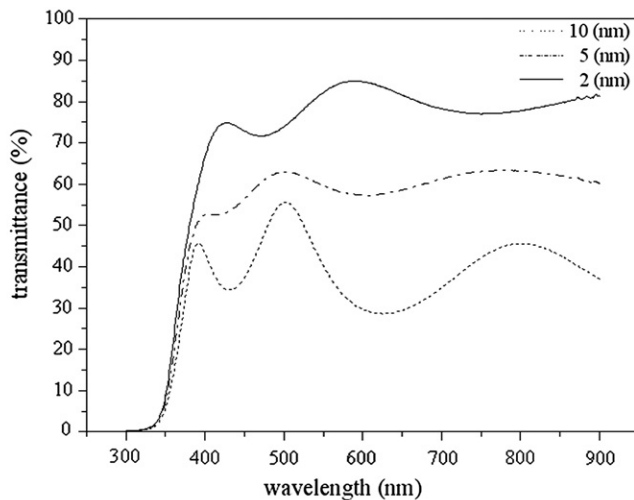

Fig. 10. Optical transmittance for AZO films as a function of Al buffer thickness, with the AZO films' thickness was 250 nm and the sputter pressure was 2.0 Pa.

of 2.0 Pa. This figure reveals that the AZO thickness increases from 250 to 450 nm, the electrical resistivity decreases from 2.22×10^{-3} to 1.61×10^{-3} Ω-cm. These results are consistent with the SEM micrographs of AZO films observed in Fig. 5. It is clear that the average gain sizes of the films differ from one another. From the micrographs, an obvious increase of grain size is observed when the AZO thickness increases from 250 to 450 nm. The larger crystallite size results can cause a decrease in grain boundary scattering and an increase of carrier lifetime [10], and consequently leads to an increase of conductivity. On the other hand, with increasing AZO thickness up to a value of 450 nm, the optical transmittance decreases to a value approximately of 72% (see Fig. 4).

Fortunato et al. [11] showed that the buffer layer between the film and the substrate improved the quality of the film. In this study, the Al thin films were grown on glass substrates at room temperature as buffer layers. The rf power was 50 W, and the thicknesses of the Al buffers were 2, 5, and 10 nm, respectively (experimental conditions are listed in Table 2). Fig. 6 presents the resistivity of the AZO films grown on Al/glass and glass as a function of buffer thickness, with the AZO film thickness of 250 nm and a sputtering pressure of 2.0 Pa. It is evident that the resistivity of the AZO films grown on Al/glass decreased as the Al buffer thickness increased. Fig. 7 (a) shows the XRD patterns of the AZO films at various Al buffer thicknesses. All the films show that the AZO films had the hexagonal ZnO wurtzite structure with a preferential orientation along the c-axis perpendicular to the substrate surface. For buffer thicknesses of 10 nm, the diffraction peaks of AZO films became sharper and more intense. This is due to the increase of crystallite size and the improvement of the crystallinity of the films. In Fig. 7 (b) and (c), the variations in the grain size and the (0 0 2) peak position are plotted as a function of the Al buffer thickness. The average grain size was the largest for the Al buffer thickness of 10 nm. The (0 0 2) peak position also showed dependence on the buffer thickness. The cross-section of the films was also revealed by SEM (Fig. 8). The films were very compact, homogeneous, perfectly adherent to the substrate, and the AZO film consists of columnar-structured grains, possibly representing the oriented grains. Atomic force micrographs of the surface morphology of the films deposited at various buffer thicknesses are shown in Fig. 9. As mentioned above, the AZO grain size increased with increased buffer thickness, and the electrical resistivity was reduced. In addition, the thickness of the Al-metal layer was not allowed beyond a certain threshold for high transmittance. With increasing thickness of the metal layer, the transmittance decreased and the reflection increased as the film became a mirror [12,13]. Fig. 10 shows the optical transmittance for AZO films with different Al buffer thicknesses. It can be seen that the transmittance decreases with an increase of the Al buffer thickness.

4. Conclusions

Transparent conducting Al-doped zinc oxide films were fabricated on soda-lime glass substrates by using rf magnetron sputtering at room temperature. The sputtering pressure dependence of the structural, morphological, electrical, and optical properties of the films was studied. As the sputtering pressure increased, the AZO thin film crystalline quality, conductivity and transmittance were promoted. All of the AZO films grown on Al/glass and glass under various sputtering pressures had strong c-axis (002) preferred orientation. The AZO films crystalline quality and resistivity were improved with increased Al buffer thickness but the film transmittance was not in good agreement with the increase in buffer thickness.

References

[1] Hao XT, Ma J, Zhang DH, Yang YG, Ma HL, Cheng CF, et al. Materials Science and Engineering B 2002;90:50–4.
[2] Nakamura T, Yamada Y, Kusumori T, Minoura H, Muto H. Thin Solid Films 2002;411:60–4.
[3] Cheong KY, Muti N, Ramanan SR. Thin Solid Films 2002;410:142–6.
[4] Lin YC, Chen MZ, Kuo CC, Yen WT. Colloids and Surfaces A: Physicochemical and Engineering Aspects 2009;337:52.
[5] Ko H, Tai WP, Kim KC, Kim SH, Suh SJ, Kim YS. Journal of Crystal Growth 2005;277:352–8.
[6] Kluth O, Schöpe G, Rech B, Menner R, Oertel M, Orgassa K, et al. Thin Solid Films 2006;502:311–6.
[7] Fernández S, Martínez-Steele A, Gandía JJ, Naranjo FB. Thin Solid Films 2009;517:3152–6.
[8] Ma QB, Ye ZZ, He HP, Zhu LP, Zhao BH. Materials Science in Semiconductor Processing 2007;10:167–72.
[9] Wei XQ, Zhang ZG, Liu M, Chen CS, Sun G, Xue CS, et al. Materials Chemistry and Physics 2007;101:285–90.
[10] Lv M, Xiu X, Pang Z, Dai Y, Han S. Applied Surface Science 2005;252:2006–11.
[11] Fortunato E, Goncalves A, Assuncao V, Marques A, Aguas H, Pereira L, et al. Thin Solid Films 2003;442:121–6.
[12] Sahu DR, Huang JL. Thin Solid Films 2006;515:876–9.
[13] Kim YS, Park JH, Choi DH, Jang HS, Lee JH, Park HJ, et al. Applied Surface Science 2007;254:1524–7.